

FAST TRACK COMMUNICATION

Gas–liquid phase coexistence in a tetrahedral patchy particle model

Flavio Romano¹, Piero Tartaglia^{1,2} and Francesco Sciortino^{1,3}¹ Dipartimento di Fisica, Università di Roma, La Sapienza, Piazzale Aldo Moro 2, 00185 Roma, Italy² INFN–CNR–SMC, Università di Roma, La Sapienza, Piazzale Aldo Moro 2, 00185 Roma, Italy³ INFN–CNR–SOFT, Università di Roma, La Sapienza, Piazzale Aldo Moro 2, 00185 Roma, Italy

Received 14 March 2007, in final form 30 May 2007

Published 27 June 2007

Online at stacks.iop.org/JPhysCM/19/322101**Abstract**

We evaluate the location of the gas–liquid coexistence line and of the associated critical point for the primitive model for water (PMW), introduced by Kolafa and Nezbeda (1987 *Mol. Phys.* **61** 161). Besides being a simple model for a molecular network forming liquid, the PMW is representative of patchy proteins and novel colloidal particles interacting with localized directional short-range attractions. We show that the gas–liquid phase separation is metastable, i.e. it takes place in the region of the phase diagram where the crystal phase is thermodynamically favoured, as in the case of particles interacting via short-range attractive spherical potentials. We do not observe crystallization close to the critical point. The region of gas–liquid instability of this patchy model is significantly reduced as compared to that from equivalent models of spherically interacting particles, confirming the possibility of observing kinetic arrest in a homogeneous sample driven by bonding as opposed to packing.

(Some figures in this article are in colour only in the electronic version)

1. Introduction

This article presents a detailed numerical study of the critical point and gas–liquid coexistence of a model introduced several years ago by Kolafa and Nezbeda [1] as a primitive model for water (PMW). The water molecule is described as a hard sphere with four interaction sites, arranged on a tetrahedral geometry, which are meant to mimic the two hydrogens and the two oxygen lone pairs of the water molecule. The PMW has been studied in detail in the past, since it is both a valid candidate for testing theories of bond association [2–8] and a model able to reproduce the thermodynamic anomalies of water [1, 9–12]. The Wertheim theory [2, 3] has been carefully compared to numerical studies, suggesting a good agreement between theoretical predictions and numerical data in the temperature (T) region where no significant ring formation is observed [11, 12]. More recently, the slow dynamics of this model has been

studied using a newly developed code for event-driven dynamics of patchy particles [12]. It has been shown that, at low density, there are indications of a gas–liquid phase separation. At intermediate density, the system can be cooled down to the smallest temperatures at which equilibration is feasible with present-day computational facilities without any signature of phase separation. In this region, the dynamics progressively slows down, following an Arrhenius law, consistently with the expected behaviour of strong network-forming liquids.

This primitive model, besides its interest as an elementary model for water, is also representative of a larger class of models which are nowadays receiving considerable interest, namely models of particles interacting with localized directional short-range attractions. This class of models also includes, apart from network-forming molecular systems, proteins [13–16] and newly designed colloidal particles [17]. Recently, the phase diagram of patchy particles has been studied [18] in an attempt to estimate the role of the surface patchiness in dictating their dynamic and thermodynamic behaviour. It has been suggested that the number of possible bonds, M , as opposed to the fraction of surface with attractive interactions, is the key ingredient in determining the width of the unstable region of the phase diagram [19–21]. A study of the evolution of the critical point on decreasing M shows a clear monotonic trend [18] and, more importantly, in the direction of decreasing critical packing fraction. Such a trend is not observed in spherical potentials on decreasing the attraction range. Thus, in low-valence particle systems, a window of packing fraction ϕ values opens up in which it is possible to reach very low T (and hence states with extremely long bond lifetimes) without encountering phase separation. This favours the establishment of a spanning network of long-living bonds, which in the colloidal community provides indication of gel formation but which, in the field of network-forming liquids, would be rather classified as glass formation [22].

As previously mentioned, we present here an accurate estimate of the location of the critical point for the PMW (for which $M = 4$), based on finite-size scaling, and of the associated gas–liquid coexistence phase diagram. Comparing with the known fluid–crystal phase coexistence loci [11], we are able to show that the gas–liquid phase separation is metastable as compared to the crystal state. Despite its metastability, we have never observed crystallization, not even close to the critical point, an observation which could be of relevance in the case of the crystallization of patchy proteins or colloids. We also show that the number density ρ of the liquid phase at coexistence is comparable to the crystal (diamond) density, much smaller than the characteristic liquid density observed in systems of particles interacting through spherically symmetric potentials.

2. The model

In the PMW, each particle is composed by a hard sphere of diameter σ and four additional sites arranged according to a tetrahedral geometry (see figure 1). Two of these sites, the proton sites H, are located on the surface of the hard sphere, i.e. at distance 0.5σ from the centre of the particle, while the two remaining sites, the lone-pair sites LP, are placed within the hard sphere at a distance 0.45σ from its centre. Besides the hard-sphere interaction, preventing different particles from exploring relative distances smaller than σ , only the H and LP sites of distinct particles interact via a square-well (SW) potential u_{SW} of width $\delta = 0.15\sigma$ and depth u_0 , i.e.

$$u_{\text{SW}}(r) = \begin{cases} -u_0 & r < \delta \\ 0 & r \geq \delta, \end{cases} \quad (1)$$

where r is here the distance between H and LP sites. We remark that the choice $\delta = 0.15\sigma$ guarantees that multiple bonding cannot take place at the same site.

3. Simulations

Three types of Monte Carlo simulation (Metropolis Grand Canonical, GCMC, Umbrella Sampling Grand Canonical, US-GCMC, and Gibbs Ensemble, GEMC) have been performed, with the aim of locating the critical point of the model, assessing the consistency with the three-dimensional Ising universality class and evaluating the gas-liquid coexistence curve. Throughout the remaining sections, we use u_0 as the energy scale, σ as the length scale and reduced units in which $k_B = 1$, thus measuring T and the chemical potential μ in units of u_0/k_B and u_0 respectively.

We define a Monte Carlo (MC) step as an average of N_Δ attempts to translate and rotate a randomly chosen particle and an average N_N attempts to insert or remove a particle. The translation in each direction is uniformly chosen between ± 0.05 and the rotations are performed around a random axis of an angle uniformly distributed between ± 0.1 rad. Unless otherwise stated, $N_\Delta/N_N = 500$. The choice of such a large ratio between translation/rotation and insertion/deletion attempts is dictated by the necessity of ensuring a proper equilibration at fixed N . This is particularly important in the case of particles with short-range and highly directional interactions, since the probability of inserting a particle with the correct orientation and position for bonding is significantly reduced as compared to the case of spherical interactions.

3.1. Critical point estimate and finite size scaling analysis

The location of the critical point was performed through the comparison of the probability distribution of the ordering operator \mathcal{M} at the critical point with the universal distribution characterizing the Ising class [23]. The ordering operator \mathcal{M} of the gas-liquid transition is a linear combination $\mathcal{M} \sim \rho - su$, where ρ is the number density, u is the energy density of the system, and s is the field-mixing parameter. Exactly at the critical point, fluctuations of \mathcal{M} are found to follow a known universal distribution, i.e. apart from a scaling factor, the same that characterizes the fluctuations of the magnetization in the Ising model [23]. Finite-size scaling (FSS) analysis has been performed to test if the PMW model belongs to the three-dimensional Ising class. Recent applications of this method to soft matter can be found in [24–26].

To locate the critical point we perform, at each size, GCMC simulations, i.e. at fixed T , μ and volume V . We follow the standard procedure of tuning T and μ until the simulated system shows ample density fluctuations, signalling the proximity of the critical point. Once a reasonable estimate of the critical point in the (T, μ) -plane has been reached, we start at least ten independent GCMC simulations to improve the statistics of the fluctuations in the number of particles N in the box and in the potential energy E .

The precise evaluation of the critical temperature and chemical potential at all system sizes is performed by a fitting procedure associated to histogram reweighting. We briefly recall [27] that this technique allows us to predict, from the joint distribution $P(N, E; T, \mu)$ of finding N particles with potential energy E at temperature T and chemical potential μ obtained from a simulation, the distribution at a different T' and μ' through the ratio of the Boltzmann factors as follows:

$$\frac{P(N, E; \mu', T')}{P(N, E; \mu, T)} \sim \frac{e^{-\beta'E} e^{\beta'\mu'N}}{e^{-\beta E} e^{\beta\mu N}} \sim e^{(\beta-\beta')E} e^{(\beta'\mu' - \beta\mu)N}, \quad (2)$$

where the proportionality constant can be calculated imposing the normalization of $P(N, E; \mu', T')$. The reweighting procedure offers reliable results provided T' and μ' are within a few per cent of T and μ .

We implement a least-squares fit procedure to evaluate the values of T , μ and s for which the reweighted distribution of \mathcal{M} is closest to the known form for Ising-like systems [28]. The result of the fit provides the best estimate for the critical temperature T_c , the critical chemical potential μ_c and s . The location of the critical point has been performed for boxes of sizes 6 through 9, corresponding to an average number of particles ranging from about 60 to over 400. The simulations for larger boxes were started at the critical parameters calculated for the closer smaller box. The $L = 9$ simulation required about one month of CPU time for each of the ten studied replicas on a 2.8 GHz Intel Xeon.

3.2. Phase coexistence

We have calculated the phase coexistence curve using US-GCMC and GEMC simulations. The US-GCMC method is a natural extension of the standard GCMC method used to locate the critical point discussed above. Once the density fluctuations at the critical point have been evaluated, one can again apply the histogram reweighting method to predict the shape of the density fluctuations at $T < T_c$ for any fixed μ value. The value of μ for which coexistence between a gas and a liquid phase is present is chosen by selecting the value μ_x for which the areas underneath the two peaks of the distribution of particle number $P(N)$ are equal.

We stress that performing a standard (Metropolis) GCMC simulation at a temperature even a few per cent lower than T_c is not feasible, due to the large free-energy barrier separating the two phases which would prevent the simulated system from sampling both liquid and gas configurations, thus yielding physically meaningless results. Several techniques have been developed to overcome this problem, among which is the Umbrella Sampling Monte Carlo method [29], which has been used to perform the calculations presented herein. The US is a biased sampling technique which aims to flatten the free-energy barrier between the two phases modifying the standard GCMC insertion/removal [30] probabilities as follows:

$$\begin{aligned} P_{\text{ins}}^{\text{US-GCMC}} &= P_{\text{ins}}^{\text{GCMC}} \frac{w(N)}{w(N+1)} \\ P_{\text{rem}}^{\text{US-GCMC}} &= P_{\text{rem}}^{\text{GCMC}} \frac{w(N)}{w(N-1)}. \end{aligned} \quad (3)$$

In these last equations $w(N)$ is a forecast on the real probability of finding N particles $P(N)$ which we have repeatedly extracted from previous higher- T simulations through the histogram reweighting technique. If the predicted probability distribution $w(N)$ is a good approximation to the real $P(N)$, the resulting biased probability will result in being flat in N and the system will thus not experience any difficulty in crossing the barrier between the liquid and gas phase. As shown in [29], the unbiased probability distribution can be easily recovered by adding a reverse bias to the results obtained with the insertion/removal probability in equation (3).

Starting from the critical point, we evaluate the phase diagram by iterating the above procedure, progressively lowering T down to the point where equilibration is not achieved any longer. Indeed, on cooling, due to the formation of a well-connected tetrahedral network, the dynamics in the liquid side slows down considerably [12]. We have been very careful in progressively increasing the ratio N_{Δ}/N_N to compensate for the slowing down of the dynamics and the extremely slow equilibration times of the liquid phase. At the lower T , $N_{\Delta}/N_N = 10\,000$. This sets a bound on the smallest T which can be investigated.

We have also implemented a Gibbs Ensemble evaluation of the phase diagram. The GEMC method was designed [31] to study coexistence in the region where the gas-liquid free-energy barrier is sufficiently high to avoid crossing between the two phases. Since nowadays this is a standard method in computational physics, we do not discuss it here and limit ourselves to noting that also in this case it is important to progressively increase, on cooling, the ratio

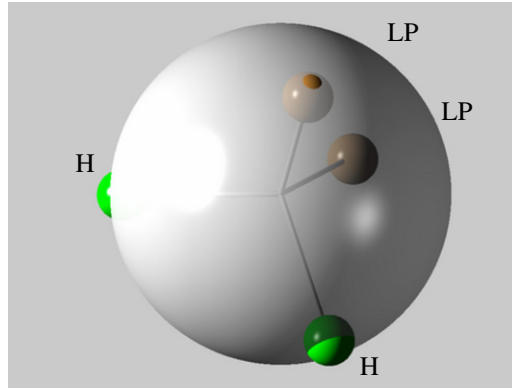


Figure 1. Pictorial representation of the model studied. Each particle is modelled as a hard-core sphere (grey large sphere of diameter σ). The four interaction sites are located in a tetrahedral arrangement. Two of the sites (the H sites, in green) are located on the surface whereas the remaining two sites (LP, in brown) are located inside the sphere, at distance 0.45σ from the centre. Only H sites and L sites on different particles interact with a square-well interaction of depth u_0 and width $\delta = 0.15\sigma$.

N_{Δ}/N_N to account for the slow dynamics characterizing the liquid state. We have studied a system of (total) 350 particles which partition themselves into two boxes whose total volume is $2868\sigma^3$, corresponding to an average density of $\rho = 0.122$. At the lowest T this corresponds to roughly 320 particles in the liquid box (of side $\approx 8\sigma$) and about 30 particles in the gas box (of side $\approx 13\sigma$). Equilibration at the lowest reported T required about three months of computer time.

4. Results

We start by showing the distributions of the ordering operator fluctuations at the (apparent) critical point for all studied sizes. Implementing the fitting procedure described in section 3.1, using histogram reweighting, we first evaluate the values of the critical parameters and the shape of the density fluctuations at the critical point. The resulting distributions, for all investigated L , are shown as a function of the scaled variable $x \equiv a_M^{-1} L^{\beta/\nu} (\mathcal{M} - \mathcal{M}_c)$ in figure 2. Here ν is the critical exponent of the correlation length and β is critical exponent of the order parameter. Within the $d = 3$ Ising universality class $\nu = 0.629$ and $\beta = 0.326$. From the fits we find that the non-universal amplitude is $a_M^{-1} = 0.34$ (independent of L). The size dependence of T_c and μ_c for $L = 6-9$ is shown in figure 3. Finite-size scaling predicts $T_c \sim L^{-(\theta+1)/\nu}$ and $\mu_c \sim L^{-(\theta+1)/\nu}$, where $\theta = 0.54$ is the universal correction to the scaling exponent [23]. Figures 3(a) and (b) show that the size dependence of the critical parameters is consistent with the expected universality class. By extrapolating the observed size dependence to $L \rightarrow \infty$ it is possible to provide an estimate for the bulk behaviour of the PMW potential. We find $T_c^{\text{bulk}} = 0.1083 \pm 0.0001$, $\mu_c^{\text{bulk}} = -1.265 \pm 0.001$. Figure 3(c) shows the L dependence of ρ_c^* , the latter being the system density (evaluated via histogram reweighting for each size) at T_c^{bulk} and μ_c^{bulk} . Finite-size scaling predicts $\rho_c^* \sim L^{-(d-1)/\nu}$. The resulting L dependence of ρ_c^* is consistent with the theoretical prediction, despite the fact that ρ_c^* data are the noisiest, since the estimate of density is the most delicate and the error is at least of the order of one particle over the volume. The field-mixing parameter s has been difficult to infer precisely due to its small value and to the discrete nature of the square-well interactions which makes

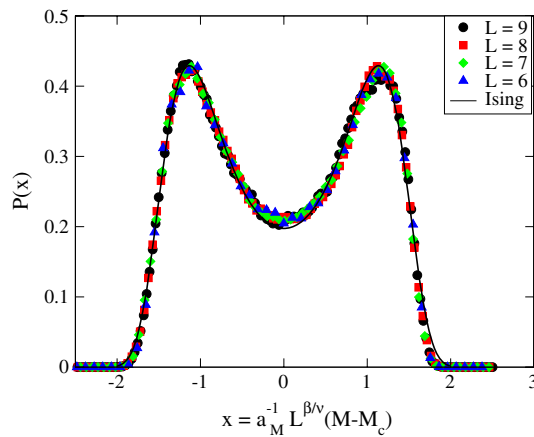


Figure 2. Probability distribution of the ordering operator for all studied sizes at the apparent critical point. The factor $a_M^{-1} = 0.34$ has been chosen to scale $P(x)$ to unit variance. The theoretical curve for the Ising model (full line) is from [28].

the distribution of N and E quantized over integer numbers. A value of $s \approx 0.07$, consistent with the results reported in [18] for a similar model, allows a simultaneous fit of all distribution functions, independently from L .

Next we discuss the gas–liquid coexistence curve for the PMW. Since only close to the critical point are size effects relevant, we have performed the calculations at $L = 6$. Figure 4 shows the behaviour of the density fluctuations $P(\rho)$ (in log scale), evaluated with US–GMC simulations (see section 3.2) along the coexistence curve. The difference between the peak and the valley in $\ln[P(\rho)]$ is a measure, in units of $k_B T$, of the activation free energy $F_{\text{barrier}}/k_B T$ needed to cross from the gas to the liquid phase and vice versa, as discussed in [37]. At the lowest studied temperature, the barrier reaches a value of about $20 k_B T$, which would clearly be impossible to overcome without the use of a biased sampling technique. Figure 4 also shows the T dependence of the barrier height, which indeed becomes of the order of the thermal energy close to the critical point.

The phase diagram resulting from our calculations is reported in figure 5(a). Both US–GMC and GEMC data are reported, showing a perfect agreement for all studied T proving that, despite the long equilibration times required, an accurate determination of the phase diagram for this model of patchy particles can nowadays be achieved. Figure 5(b) shows the same data, together with the fluid–crystal coexistence lines calculated by Vega and Monson [11] and complemented with the bond percolation line from [12]. We also report in the graph a so-called iso-diffusivity line, i.e. the set of points in the T – ρ plane in which the diffusion coefficient D is constant. By selecting the smallest value of D which can be calculated with the present time computational facilities, the iso-diffusivity line provides an estimate of the shape of the glass line. Figure 5 also shows the coexistence curve evaluated from the Wertheim theory, from [11].

Several observations arise from the data in figure 5. First of all, we observe that the critical point, as well as the liquid branch of the coexistence curve, is characterized by a percolating (but transient) structure of bonds between pairs of H and LP. This is not unexpected, since the propagation of infinite-range correlations, characteristic of a critical point, does require the presence of a spanning cluster [32]. Particle diffusion is still significant, despite the presence of the transient percolating network of bonds, as shown by the comparison between the phase

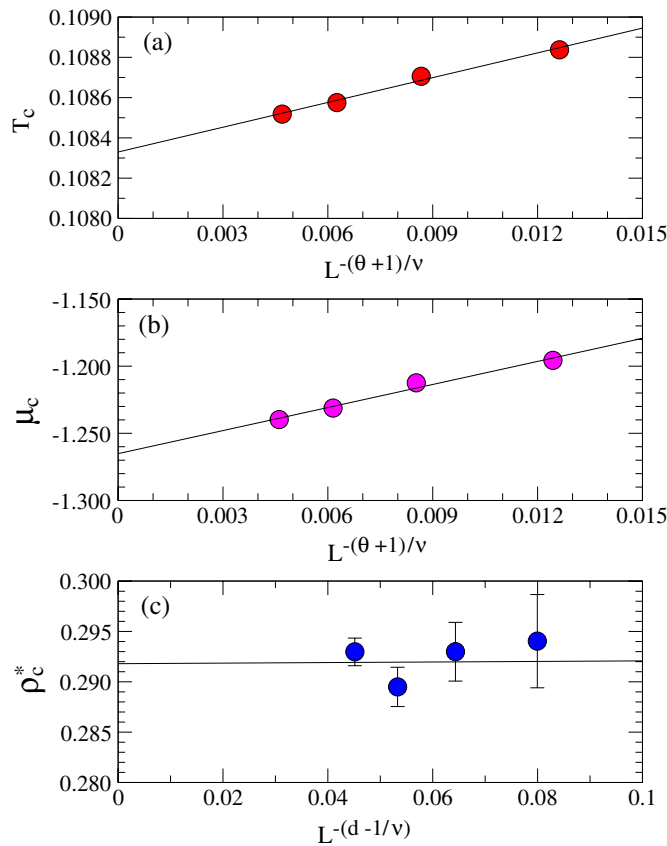


Figure 3. Size dependence of the apparent critical temperature $T_c(L)$ (a), the apparent critical chemical potential $\mu_c(L)$ (b) and the density at the true critical point $\rho_c^*(L)$ (c).

coexistence and the small- D iso-diffusivity line. In the region of T where the dynamics becomes so slow that equilibration can not be achieved on the present computational timescale, it becomes impossible also to evaluate the gas–liquid coexistence.

The gas–liquid coexistence is found to be metastable with respect to fluid–crystal coexistence, in analogy with the case of particles interacting through spherical short-range potentials. This notwithstanding, we never observe crystallization close to the critical point. This suggests that the increase in local density brought about by the critical fluctuations does not sufficiently couple with the orientational ordering required for the formation of the open diamond crystal structure.

The comparison between the GEMC and US–GCMC simulation phase diagram with the theoretical predictions of the Wertheim theory suggests that the latter provides a quite accurate estimate for T_c , whereas the ρ dependence is only approximate. Indeed, the Wertheim theory predicts a vapor–liquid critical point at $T_c = 0.1031$ and $\rho_c = 0.279$ [11]. These differences between theoretical predictions and numerical data confirm the conclusions that have previously been reached for models of patchy particles with different numbers of sticky spots [18].

Finally, we note that in a very limited T interval (less than 10% of T_c), the liquid density approximately reaches a value comparable to the diamond crystal density, which for the present

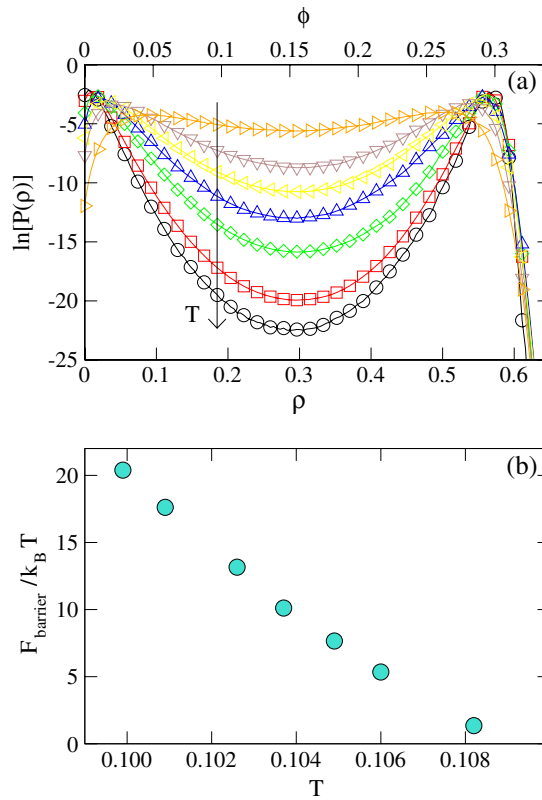


Figure 4. (a) Logarithm of the distribution of density fluctuations $P(\rho)$ at $T = 0.1082, 0.1060, 0.1049, 0.1037, 0.1026, 0.1009, 0.0999$, providing the negative of the density dependence of the free energy. The difference between the value of $P(\rho)$ at the valley and at the top is a measure of the free-energy barrier that needs to be overcome to cross from the gas to the liquid state or vice versa [37]. (b) Free-energy barrier (in units of $k_B T$) between gas and liquid versus T at coexistence.

model has been calculated [11] as $0.4880 < \rho < 0.6495$. Thus, as for the crystal state, the density of the liquid phase at coexistence is rather small, approximately a factor of two smaller as compared to the case of spherically interacting particles.

Finally, for the sake of completeness we show in figure 6 the location of the gas–liquid coexistence in the μ – T plane.

5. Conclusions

In this article we have presented an accurate determination of the critical point and of the gas–liquid phase coexistence curve for a primitive model for water, introduced by Kolafa and Nezbeda [1]. Despite its original motivation, the PMW can also be studied as a model for patchy colloidal particles and, perhaps, as an elementary model for describing patchy interactions in proteins. To this extent, it is particularly important to understand the qualitative features of the phase diagram, the stability or metastability of the gas–liquid line and the propensity to crystallize.

We have shown that the critical fluctuations are consistent with the Ising universality class, both via the analysis of the shape of the density distribution and via the size dependence of

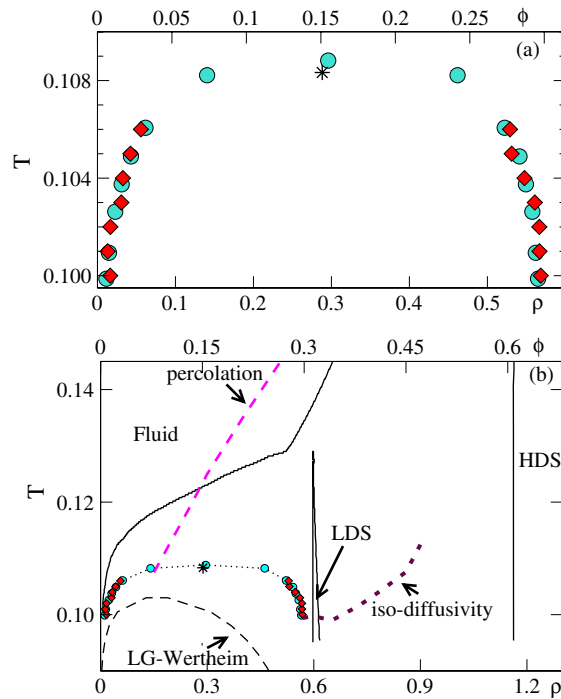


Figure 5. (a) Calculated gas–liquid coexistence for the PMW. Both GEMC (diamonds) and US-GCMC for $L = 6$ (circles) simulation results are shown. The star indicates the bulk ($L \rightarrow \infty$) critical point estimate. (b) Extended phase diagram for the PMW, including: (i) the theoretical (Wertheim) gas–liquid coexistence line (dashed), (ii) the field of stability of the fluid, of the high-density crystal (HDS) and of the low-density crystal (LDS) phases from [11]; (iii) an iso-diffusivity line (for the smallest investigated value of D) from [12]; (iv) percolation line from [12].

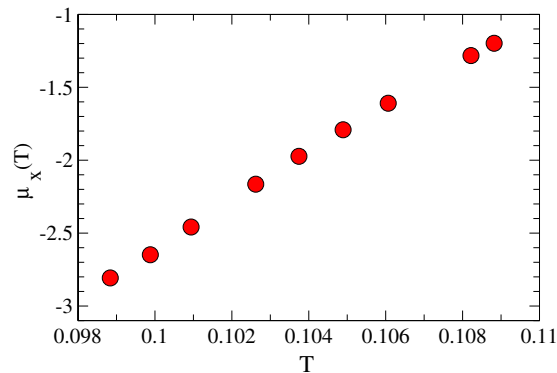


Figure 6. Chemical potential at coexistence μ_x for $L = 6$.

the critical parameters. The determination of the critical point allows us to prove that, for the present model, the liquid phase is not present in equilibrium, and it is only observed in a metastable condition. In the case of the square-well spherical interaction potentials, the thermodynamic stability of the gas–liquid critical point is achieved when the range of the interaction potential becomes one quarter of the particle diameter [33, 35, 36]. Data reported in

this article (see figure 5) confirm that the property of short-range potentials of missing a proper equilibrium liquid phase is retained in short-range patchy particles. It would be of interest to study for which critical value of the interaction range a proper liquid phase appears in patchy particle models.

The evaluation of the gas–liquid coexistence has been performed using two distinct methods, the US–GCMC and the GEMC, and a very good agreement has been recorded despite the difficulties in equilibrating the liquid phase at low T . The present results, together with previous studies of the crystal phase and of the slow low- T dynamics, offer a coherent picture of the behaviour of the model. It is shown that phase separation is intervening only at low T for $\rho \lesssim 0.6$, a value significantly smaller than the corresponding value for spherical interaction potentials. This is consistent with the fact that the number of attractive interactions in which a particle can be engaged (four in the present model) controls the minimum density of the liquid phase. These results elucidate the different nature of bonded liquids (the so-called network forming) with respect to the category of spherically interacting liquids. For bonded systems, there is an intermediate region, between the high-density packed structure and the unstable region, in which gas–liquid phase separation is observed, which is not accessible to spherically interacting particles. In this intermediate-density region, the system is structured in a percolating network and both static and dynamic quantities are controlled by the presence of bonds. This picture, which has been developing in a progression of studies [12, 19, 22, 34], is confirmed by the present results.

Acknowledgments

We acknowledge support from MIUR-Prin and MCRTN-CT-2003-504712.

References

- [1] Kolafa J and Nezbeda I 1987 Monte Carlo simulations on primitive models of water and methanol *Mol. Phys.* **61** 161–75
- [2] Wertheim M S 1984 Fluids with highly directional attractive forces. I. Statistical thermodynamics *J. Stat. Phys.* **35** 19–34
- [3] Wertheim M S 1984 Fluids with highly directional attractive forces. II. Thermodynamic perturbation theory and integral equation *J. Stat. Phys.* **35** 35–47
- [4] Ghonasci D and Chapman W G 1993 Theory and simulation for associating fluids with four bonding sites *Mol. Phys.* **79** 291–311
- [5] Sear R P and Jackson G 1996 Thermodynamic perturbation theory for association with bond cooperativity *J. Chem. Phys.* **105** 1113–20
- [6] Duda Y, Segura C J, Vakarin E, Holovko M F and Chapman W G 1998 Network forming fluids: integral equations and Monte Carlo simulations *J. Chem. Phys.* **108** 9168–76
- [7] Peery T B and Evans G T 2003 Association in a four-coordinated, water-like fluid *J. Chem. Phys.* **118** 2286–300
- [8] Kalyuzhnyi Y V and Cummings P T 2003 Yukawa sticky m-point model of associating fluid *J. Chem. Phys.* **118** 6437–45
- [9] Nezbeda I, Kolafa J and Kalyuzhnyi Y V 1989 Primitive model of water. II. Theoretical results for the structure and the thermodynamic properties *Mol. Phys.* **68** 143–60
- [10] Nezbeda I and Iglesias-Silva G A 1990 Primitive model of water. III. Analytic theoretical results with anomalies for the thermodynamic properties *Mol. Phys.* **69** 767–74
- [11] Vega C and Monson P A 1998 Solid–fluid equilibrium for a molecular model with short ranged directional forces *J. Chem. Phys.* **109** 9938–49
- [12] De Michele C, Gabrielli S, Tartaglia P and Sciortino F 2006 Dynamics in the presence of attractive patchy interactions *J. Phys. Chem. B* **110** 8064–79
- [13] Lomakin A, Asherie N and Benedek G B 1999 Aeolotopic interactions of globular proteins *Proc. Natl Acad. Sci.* **96** 9465–8
- [14] Sear R P 1999 Phase behaviour of a simple model of globular proteins *J. Chem. Phys.* **111** 4800–6

- [15] Kern N and Frenkel D 2003 Fluid–fluid coexistence in colloidal systems with short-ranged strongly directional attraction *J. Chem. Phys.* **118** 9882–9
- [16] Doye J P K, Louis A A, Lin I-C, Allen L R, Noya E G, Wilber A W, Kok H C and Lyus R 2007 Controlling crystallization and its absence: proteins, colloids and patchy models *Phys. Chem. Chem. Phys.* **9** 2197–205
- [17] Manoharan V N, Elsesser M T and Pine D J 2003 Dense packing and symmetry in small clusters of microspheres *Science* **301** 483–6
- [18] Bianchi E, Largo J, Tartaglia P, Zaccarelli E and Sciortino F 2006 Phase diagram of patchy colloids: towards empty liquids *Phys. Rev. Lett.* **97** 168301
- [19] Zaccarelli E, Buldyrev S V, La Nave E, Moreno A J, Saika-Voivod I, Sciortino F and Tartaglia P 2005 Model for reversible colloidal gelation *Phys. Rev. Lett.* **94** 218301–5
- [20] Sciortino F, Buldyrev S, De Michele C, Ghofraniha N, La Nave E, Moreno A, Mossa S, Tartaglia P and Zaccarelli E 2005 Routes to colloidal gel formation *Comput. Phys. Commun.* **169** 166–71
- [21] Zaccarelli E, Saika-Voivod I, Buldyrev S V, Moreno A J, Tartaglia P and Sciortino F 2006 Gel to glass transition in simulation of a valence-limited colloidal system *J. Chem. Phys.* **124** 4908
- [22] De Michele C, Tartaglia P and Sciortino F 2006 Slow dynamics in a primitive tetrahedral network model *J. Chem. Phys.* **125** 4710
- [23] Wilding N B 1996 Simulation studies of fluid critical behaviour *J. Phys.: Condens. Matter* **9** 585–612
- [24] Miller M A and Baxter D F 2003 *Phys. Rev. Lett.* **90** 135702
- [25] Caballero J B *et al* 2004 Oppositely charged colloidal binary mixtures: a colloidal analog of the restricted primitive model *J. Chem. Phys.* **121** 2428–35
- [26] Vink R L C and Horbach J 2004 Grand canonical Monte Carlo simulation of a model colloid–polymer mixture: coexistence line, critical behavior, and interfacial tension *J. Chem. Phys.* **121** 3253–8
- [27] Ferrenberg A M and Swendsen R H 1988 New Monte Carlo technique for studying phase transitions *Phys. Rev. Lett.* **61** 2635–8
- [28] Tsypin M M and Blöte H W J 2000 Probability distribution of the order parameter for the three-dimensional Ising-model universality class: a high-precision Monte Carlo study *Phys. Rev. E* **62** 73–6
- [29] Patey G N and Valleau J P 1975 A Monte Carlo method for obtaining the interionic potential of mean force in ionic solution *J. Chem. Phys.* **63** 2334–9
- [30] Smith B and Frenkel D 1996 *Understanding Molecular Simulations* (New York: Academic)
- [31] Panagiotopoulos A Z 1987 Direct determination of phase coexistence properties of fluids by Monte Carlo simulations in a new ensemble *Mol. Phys.* **61** 813–26
- [32] Coniglio A and Klein W 1980 Clusters and Ising critical droplets: a renormalization group approach *J. Phys. A: Math. Gen.* **13** 2775
- [33] Vliegthart G A and Lekkerkerker H N W 2000 Predicting the gas–liquid critical point from the second virial coefficient *J. Chem. Phys.* **12** 5364–9
- [34] Sastry S, La Nave E and Sciortino F 2006 Maximum valency lattice gas models *J. Stat. Mech. Theor. Exp.* **12** 10
- [35] Pagan D L and Gunton J D 2005 Phase behavior of short-range square-well model *J. Chem. Phys.* **123** 174505
- [36] Liu H, Garde S and Kumar S 2005 Direct determination of phase behavior of square-well fluids *J. Chem. Phys.* **122** 184515
- [37] Virnau P and Muller M 2004 Calculation of free energy through successive umbrella sampling *J. Chem. Phys.* **120** 10925